Available online at www.sciencedirect.com

ScienceDirect

Procedia Structural Integrity 26 (2020) 166–174

Structural Integrity Procedia

www.elsevier.com/locate/procedia

The 1st Mediterranean Conference on Fracture and Structural Integrity, MedFract1

Determination of Fatigue Limit by Static Thermographic Method and Classic Thermographic Method on Notched Specimens

Pietro Foti[a*], Dario Santonocito[b], Paolo Ferro[c], Giacomo Risitano[b], Filippo Berto[a]

[a]*Norwegian University of Science and Technology, MTP Gløshaugen, Richard Birkelands vei 2B, Trondheim 7491, Norway*
[b]*University of Messina, Departement of Engineering, Contrada di Dio (S. Agata), Messina 98166, Italy*
[c]*University of Padova, Department of Management and Engineering, Stradella San Nicola 3, Vicenza 36100, Italy*

Abstract

The aim of the present work is to investigate the possibility to evaluate the fatigue limit of such a component through the so-called Static Thermographic Method (STM). This new approach has been proposed in 2013 by Risitano and Risitano to determinate the fatigue limit of metallic materials through static tensile tests. Investigating the trend of the surface temperature of the material during static tensile test, the method proposes to correlate the first deviation from linearity of the surface temperature to a damage limit that has been proven to have relation with the fatigue limit. Static tensile tests at different stress rate have been carried out on V-notched specimens. Stepwise fatigue tests have been carried out in order to apply the classic Thermographic Method that has been hugely validated to determinate the fatigue limit of metallic components. Static tests at different stress rate showed that the method is dependent on this parameter; anyway, this dependence does not affect the results achieved in terms of fatigue limit. The experimental results showed a good agreement with the energetic methods considered in the present work.

Keywords: Fatigue assessment; Static Thermographic Method; Thermographic Method.

1. Introduction

In the field of mechanical design, the determination of the material mechanical properties is particularly time consuming especially dealing with fatigue properties whose obtainment through traditional fatigue tests requires a

* Corresponding author.
E-mail address: pietro.foti@ntnu.no

10.1016/j.prostr.2020.06.020

large number of specimens for its assessment. The infrared thermography (IR) techniques could be used to determine the material fatigue properties especially when a limited set of specimens are available or when there is the need to decrease costs and tests time. Due to these peculiarities, the IR techniques are very attractive for many researchers who face the problem of fatigue of materials.

Their use has already shown that the thermal analysis allows the estimation of the fatigue limit of the material with a very small number of specimens dealing with plain and notched steel specimens under static and fatigue tests (Amiri and Khonsari, 2010a, 2010b; Corigliano et al., 2019; Plekhov et al., 2014; Ricotta et al., 2019; Rigon et al., 2019; Risitano et al., 2014; Risitano and Risitano, 2013; Risitano and Clienti, 2012), laminated composite under tensile static loading (Colombo et al., 2012; Palumbo et al., 2017; Vergani et al., 2014), polyethylene under static and fatigue loading (Risitano et al., 2018), short glass fiber-reinforced polyamide composites under static and fatigue loading (Crupi et al., 2015b), steels under high cycle (Amiri and Khonsari, 2010b; Corigliano et al., 2019; Curà et al., 2005; Meneghetti et al., 2013) and very high cycle fatigue regimes (Crupi et al., 2015a; Plekhov et al., 2014).

Among the IR techniques, we considered in the present work the Thermographic Method (TM), first developed and used in 1986 (Curti et al., 1986) to predict the fatigue limit and the S-N curve with a very limited number of specimens tested under fatigue loading conditions (Fargione et al., 2002)., and the Static Thermographic Method (STM), proposed in 2013 (Risitano and Risitano, 2013) as a rapid and economic procedure to estimates the fatigue limit of such a material analysing the surface temperature trend of specimen subjected to static loads. More details about these two methods are given in section 2.

Nomenclature

c	specific heat capacity of the material [J/(kg.K)]
K_m	thermoelastic coefficient [MPa-1]
R	stress ratio
t	test time [s]
T, T_i	instantaneous value of the temperature [K]
T_0	initial value of temperature estimated at time zero [K]
α	thermal diffusivity of the material [m2/s]
ΔT_S	absolute surface temperature variation during a static tensile test [K]
ΔT_1	estimated value of temperature for the first set of temperature data [K]
ΔT_2	estimated value of temperature for the second set of temperature data [K]
ρ	density of the material [kg/m3]
σ, σ_i	stress level, principal stress [MPa]
σ_D	critical macro stress that produces irreversible micro-plasticity [MPa]
σ_{lim}	fatigue limit estimated with the Static Thermographic Method

2. Theoretical background

2.1. Thermographic Method

Dealing with such a component subjected to a cyclic load above its fatigue limit, the analysis of its surface temperature, detected by means of an infrared camera, shows that it is possible to distinguish three different phases as shown in figure 1 a). The first phase is characterized by a rapid increment of the surface temperature whose rate with the number of cycles increase with increasing the stress with respect to the fatigue limit. After the initial increment, the temperature reaches a stabilization value that characterize the second phase. Finally, in the third phase, the temperature starts increasing rapidly until the component failure. Both the temperature rate with the cycles of the first phase and the stabilization temperature of the second phase depends on the applied stress; in particular, the higher the stress, the higher the temperature rate and the stabilization temperature. It is worth noting that with applied stresses below the fatigue limit of the material, there still is an increase in temperature ΔT that however is usually limited and negligible considering practical applications(La Rosa and Risitano, 2000)

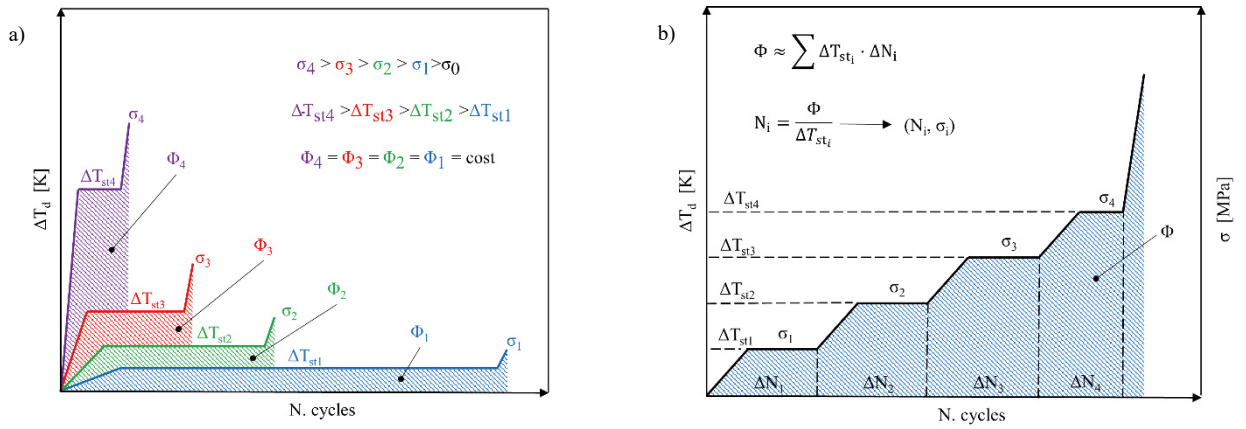

Figure 1: a) Typical T-N curves for steels under fatigue loading; b) Temperature evolution during a stepped fatigue test.

As a consequence of the properties explained in the above, it was proposed by La Rosa and Risitano (La Rosa and Risitano, 2000) that the fatigue limit could be determined by plotting the increase in temperature ΔT, or the initial thermal gradient $\Delta T/\Delta N$ against the applied load; their trends in this kind of diagram are linear and the fatigue limit σ_0 can be found as the intercept of the curve on the applied load axis ($\Delta T = 0$ or $\Delta T/\Delta N = 0$). When the increments below the fatigue limit are not negligible it is possible to notice a knee in these diagrams. The knee coordinate on the applied load axis represents the fatigue limit of the material as suggested by (Curà et al., 2005).

Another important property of the temperature trend vs the number of cycles is that the subtended area can be assumed constant despite the applied cyclical stress, given the stress ratio R and the test frequency f. The area represents an energy parameter, Φ, strictly related with the energetic release of the material.

Exploiting this property, Fargione et al. (Fargione et al., 2002) proposed a rapid test procedure that involves in a unique fatigue tests different applied stresses, in a stepped way, until the failure of the specimen (figure 1b). By knowing the Energy Parameter and the different stabilization temperature for each applied stress level, it is possible to estimate the number of cycles at which the specimen would had failed if it was cyclically loaded with that stress. Following this procedure, with at least three tests, it is possible to obtain in a rapid way the whole S-N curve of the material.

2.2. Static Thermographic Method

During a uniaxial traction test on common engineering metals, analysing the surface temperature evolution, it is possible to identify three different phases as shown in figure 2.

The first phase is characterized by an approximately linear decrease of the temperature due to the thermoelastic effect that, for linear isotropic homogeneous material in adiabatic condition, is proportional to the variation of the sum of the principal stresses following Lord Kelvin's effect:

$$\Delta T_S = -\frac{\alpha}{\rho c} T_0 \cdot (\sigma_1 + \sigma_2 + \sigma_3) \tag{1}$$

That for uniaxial test becomes:

$$\Delta T_S = -\frac{\alpha}{\rho c} T_0 \cdot \sigma_1 = -K_m \cdot T_0 \cdot \sigma_1 \tag{2}$$

A variation in the temperature trend from the linearity identifies the transition between thermoelastic and thermoplastic behavior due to the beginning of irreversible micro-plasticization in the material due to structural or superficial micro-defects; this identifies the second phase of the temperature trend. A third phase is characterized by a very high increment of the temperature until the component failure.

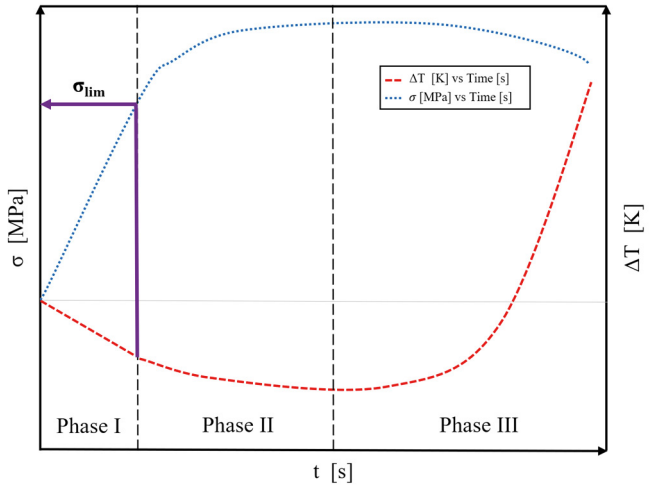

Figure 2:Typical surface temperature vs time curve

Through high precision IR sensors, it is possible to investigate the experimental temperature during the static tensile tests and correlate the point where the temperature trend deviates from the linearity with the applied stress. The Static Thermographic Method (STM), proposed by Risitano and Risitano(Risitano and Risitano, 2013) makes the assumption that cyclically applying to the component higher stress than the value identify before, at which local and irreversible plastic condition are achieved in the component, the component will have a fatigue failure. Therefore, in not conventional way, the value of the stress, at which the temperature trend deviates from the linearity of the thermoelastic behavior, is strictly related to the fatigue limit of the material.

3. Materials and Methods

Static tensile tests and steps fatigue tests, according to (Fargione et al., 2002) procedure, were carried out on specimens made of AISI 1035. The geometry of the detail is reported in figure 3.

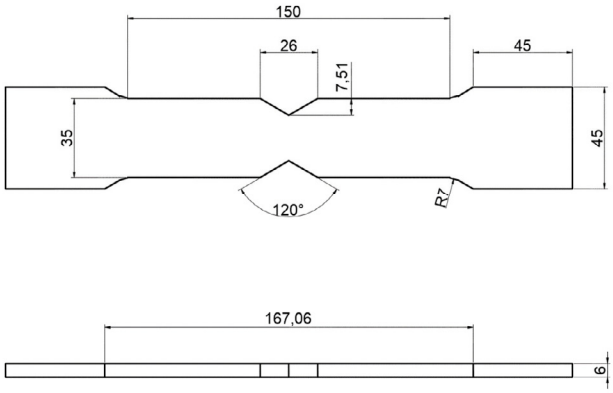

Figure 3: Tested specimen geometry (measures in mm)

All the tests were performed with a servo-hydraulic axial load machine INSTRON 8854 with maximum load capacity of 250 kN. Five static tensile tests were performed under load control. In order to better meet the adiabatic condition needed to be able to detect in the first phase of the temperature evolution the thermoelastic behavior, described by eq.2, three different load application speeds have been considered: 60 MPa / min; 120 MPa / min; 180 MPa / min . A second series of fatigue tests with stress ratio $R = -1$ and frequency $f = 20$ Hz was performed on 3 other specimens.

In particular, one of the fatigue tests was carried out with step increases of the stress amplitude, ranging from 42 MPa up to 250 MPa, with 20000 cycles per step.

In order to apply TM and STM during tensile and fatigue tests, infrared thermography was used to monitor the evolution of the surface temperature of the specimen. The infrared camera FLIR A40, with a sample rate of 1 image per second and a temperature measurement range between $-40^{\circ}C$ and $+120^{\circ}C$, was used. During all the tests, the maximum temperature value of a rectangular measurement area, placed in the vicinity of the specimen reduced section, has been recorded.Before starting the tests, the specimens were coated with a black paint, to increase the thermal emissivity of the material up to 0.98.

4. Results and Discussion

The specimen surface temperature evolution during static tensile tests has been recorded by means of an IR camera in order to apply the STM. The difference between the instantaneous temperature and the initial temperature of the surface at time zero $(\Delta T = T_i - T_0)$ has been related with the applied stress synchronizing the load data from the servo-hydraulic axial load machine with the one from the IR camera taking as reference the failure of the specimen easily detectable on both the data acquired..

In order to better identify the different phases of the surface temperature evolution and highlight the thermoelastic trend, a rlowless filter has been used to filter the data, considering a data span of 10%. In the initial part of the $\Delta T - t$ curve the thermoelastic behavior is clearly distinguishable as well as the deviation from the linearity entering in the thermoplastic region and the further rapid temperature increment before the final failure.

It is possible to draw a linear regression line to interpolate the data referred to the thermoelastic behavior, designated in the diagram as ΔT_1, and another one to interpolate the data referred to the second phase, ΔT_2 in the diagram. It is worth underlining that, in the interpolations explained above, the temperature values near the transition between the thermoelastic and the thermoplastic behavior have not been considered (Experimental Temperature series).

Solving the system of equations, it is possible to determine the intersection point of the two straight lines, whose time coordinate allows to determine the corresponding value of the applied stress, namely $\sigma_{\lim}$, that, according to the considerations already done in section 2 results to be the macroscopic stress that lead to the first plasticization phenomena in the material.

The first three static tests have been carried out at three different applied stress rates in order to find out the best condition to meet the adiabatic condition as explained in section 2. From the data acquired, shown in figure 4, it is clear that the best results are achieved with an applied stress rate of $120\ MPa/\min$ that has been chosen to carry out the remaining two static tests whose temperature evolution data are reported in figure 5.

For the other two applied stress rates the effect in terms of decrease in surface temperature seems to be mitigate; this can be addressed, for the lowest rate, to the possible exchanged heat with the surrounding environment due to the longer test time while, for the faster rate, the excessive reduced time of the test do not allow the material to manifest the temperature evolution clearly in each one of its phases. Although in some of the tests considered the temperature evolution phases are not so clearly detectable, for all the five static tensile tests it has been possible to interpolate the data according to the procedure explained above with a resulted average value for the limit stress of $\sigma_{\lim} = 175.4 \pm 5 MPa$.

During the fatigue tensile tests, the evolution of the specimen surface temperature has also been analyzed in order to apply the TM. The fatigue limit has been evaluated applying the thermographic method considering the initial thermal gradient $\Delta T/\Delta N$; from the tests carried out four initial thermal gradients were available, two from the steps fatigue tests figure 6, considering that only two of all the steps were at a stress level above the fatigue limit of the material, and two from the other fatigue tests figure 7.

A value of $\sigma_{\lim} = 174.6 MPa$ has been found, as shown in figure 8

5. Conclusion

In this work the surface temperature evolution during tensile tests on AISI 1035 has been evaluated in order to determine through the Static Thermographic Method the fatigue limit of the material and to compare it with the value obtained through the Thermographic Method applied to specimens tested under fatigue loading. The average value of

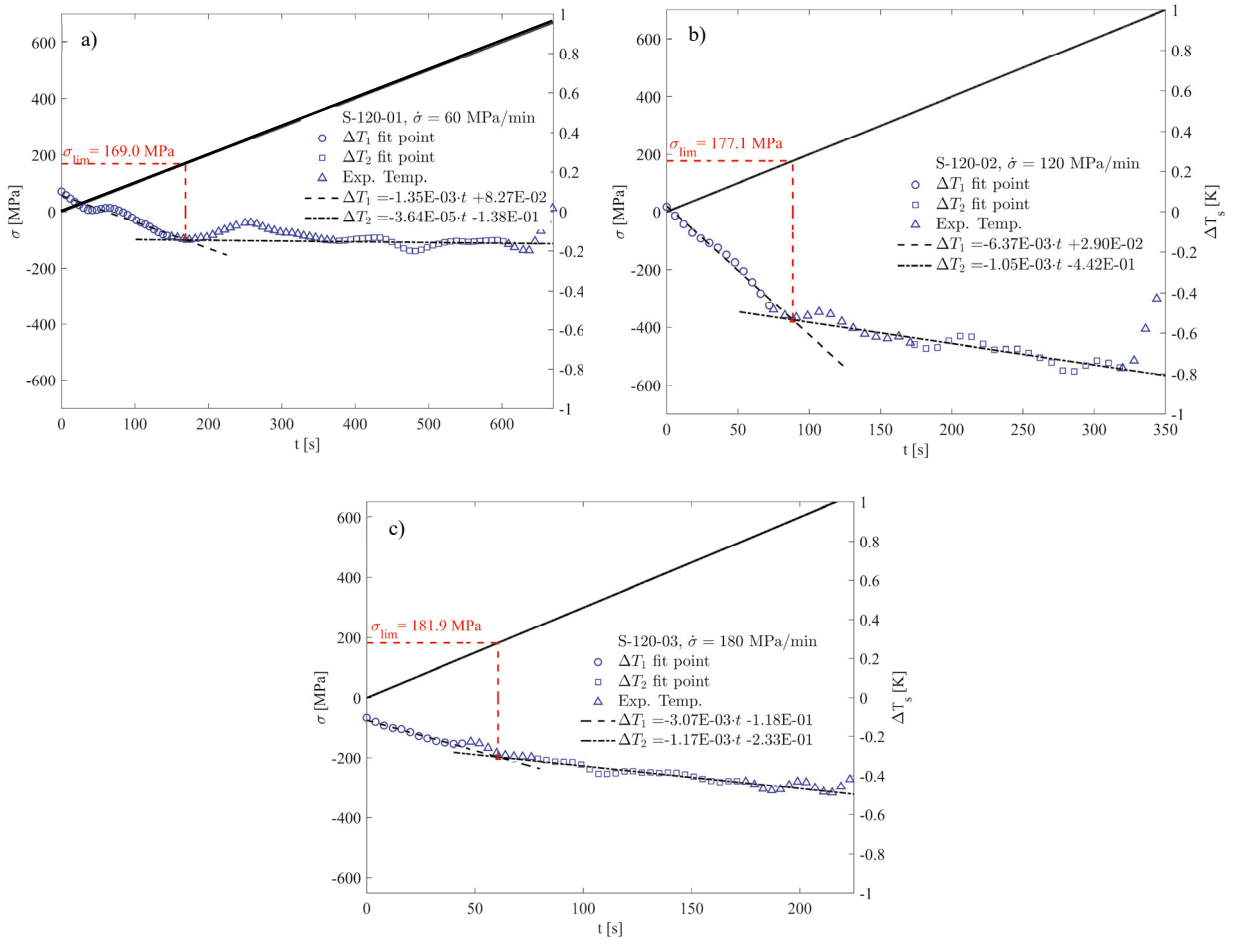

Figure 4: Surface temperature vs time trend for: a) $\dot{\sigma} = 60MPa/min$; b) $\dot{\sigma} = 120MPa/min$; c) $\dot{\sigma} = 180MPa/min$.

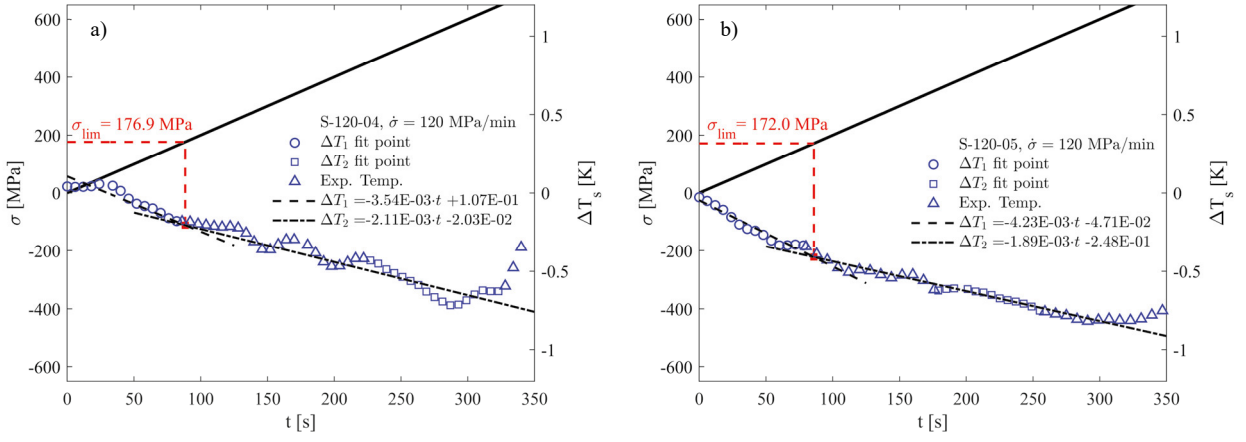

Figure 5: Surface temperature vs time trend with $\dot{\sigma} = 120MPa/min$

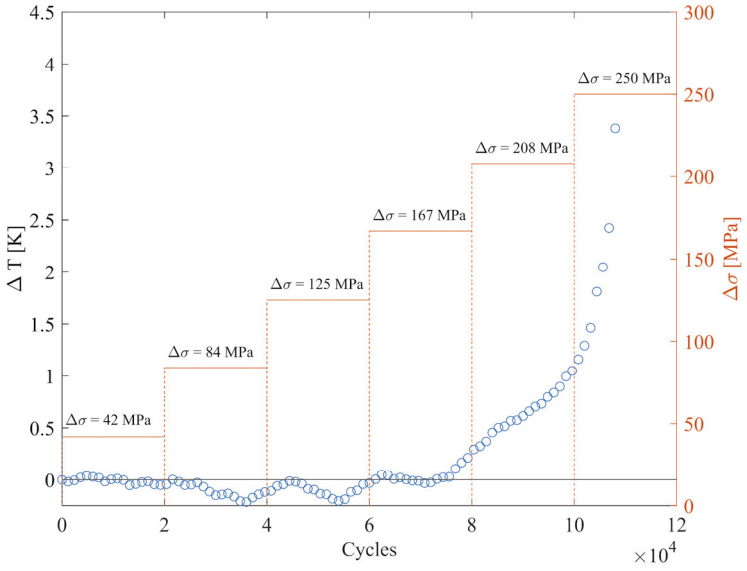

Figure 6: Surface temperature vs Cycles during a stepped fatigue test

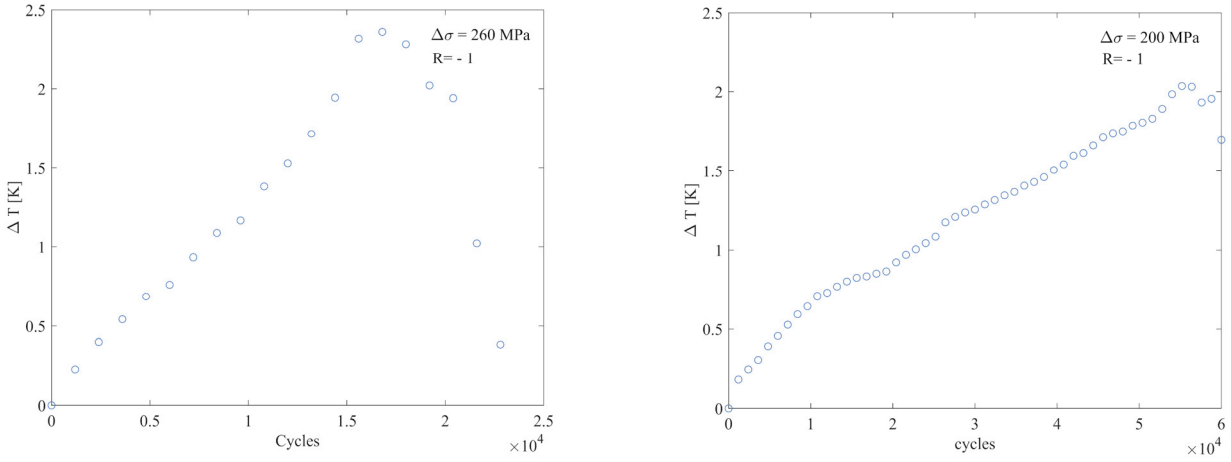

Figure 7: Surface temperature trend during fatigue tests

the limit stress evaluated through the STM as the stress level at which the temperature deviates from its linear trend is equal to $\sigma_{\lim} = 175.4 \pm 5 MPa$ while through the TM method the estimated fatigue limit value result to be $\sigma_{\lim} = 174.6 MPa$.

The predicted values by means of the two TMs are in good agreement showing that the STM, as the better proved TM, can estimate, even with a very limited number of specimens, the fatigue limit of the material.

The influence of the stress application rate on the energetic release has been evaluated and results in an higher value of the minimum acquired temperature and, therefore, in a mitigation of the investigated effect with respect to the data observed with a stress application speed that allows to better meet the adiabatic conditions; however, although this influence, the three different phases of the temperature evolutions are still easily distinguishable.

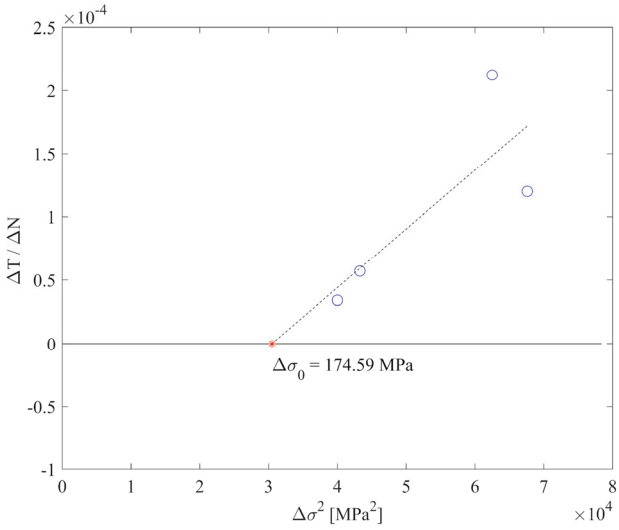

Figure 8: Application of the TM method through the initial thermal gradient

References

Amiri, M., Khonsari, M.M., 2010a. Life prediction of metals undergoing fatigue load based on temperature evolution. Mater. Sci. Eng. A 527, 1555–1559. https://doi.org/10.1016/j.msea.2009.10.025

Amiri, M., Khonsari, M.M., 2010b. Rapid determination of fatigue failure based on temperature evolution: Fully reversed bending load. Int. J. Fatigue 32, 382–389. https://doi.org/10.1016/j.ijfatigue.2009.07.015

Colombo, C., Vergani, L., Burman, M., 2012. Static and fatigue characterisation of new basalt fibre reinforced composites. Compos. Struct. 94, 1165–1174. https://doi.org/10.1016/j.compstruct.2011.10.007

Corigliano, P., Cucinotta, F., Guglielmino, E., Risitano, G., Santonocito, D., 2019. Fatigue assessment of a marine structural steel and comparison with Thermographic Method and Static Thermographic Method. FFEMS 1–10. https://doi.org/10.1111/ffe.13158

Crupi, V., Epasto, G., Guglielmino, E., Risitano, G., 2015a. Thermographic method for very high cycle fatigue design in transportation engineering. Proc. Inst. Mech. Eng. Part C J. Mech. Eng. Sci. 229, 1260–1270. https://doi.org/10.1177/0954406214562463

Crupi, V., Guglielmino, E., Risitano, G., Tavilla, F., 2015b. Experimental analyses of SFRP material under static and fatigue loading by means of thermographic and DIC techniques. Compos. Part B Eng. 77, 268–277. https://doi.org/10.1016/j.compositesb.2015.03.052

Curà, F., Curti, G., Sesana, R., 2005. A new iteration method for the thermographic determination of fatigue limit in steels. Int. J. Fatigue 27, 453–459. https://doi.org/10.1016/j.ijfatigue.2003.12.009

Curti, G., La Rosa, G., Orlando, M., Risitano, A., 1986. Analisi tramite infrarosso termico della temperatura limite in prove di fatica. Proc. XIV Convegno Naz. AIAS 211–220.

Fargione, G., Geraci, A., La Rosa, G., Risitano, A., 2002. Rapid determination of the fatigue curve by the thermographic method. Int. J. Fatigue 24, 11–19. https://doi.org/10.1016/S0142-1123(01)00107-4

La Rosa, G., Risitano, A., 2000. Thermographic methodology for rapid determination of the fatigue limit of materials and mechanical components. Int. J. Fatigue 22, 65–73. https://doi.org/10.1016/S0142-1123(99)00088-2

Meneghetti, G., Ricotta, M., Atzori, B., 2013. A synthesis of the push-pull fatigue behaviour of plain and notched stainless steel specimens by using the specific heat loss. Fatigue Fract. Eng. Mater. Struct. 36, 1306–1322. https://doi.org/10.1111/ffe.12071

Palumbo, D., De Finis, R., Demelio, P.G., Galietti, U., 2017. Early Detection of Damage Mechanisms in Composites During Fatigue Tests, in: Zehnder, A.T., Carroll, J., Hazeli, K., Berke, R.B., Pataky, G., Cavalli, M., Beese, A.M., Xia, S. (Eds.), Fracture, Fatigue, Failure and Damage Evolution, Volume 8. Springer International Publishing, Cham, pp. 133–141.

Plekhov, O., Naimark, O., Semenova, I., Polyakov, A., Valiev, R., 2014. Experimental study of thermodynamic and fatigue properties of submicrocrystalline titanium under high cyclic and gigacyclic fatigue regimes. Proc. Inst. Mech. Eng. Part C J. Mech. Eng. Sci. 229, 1271–1279. https://doi.org/10.1177/0954406214563738

Ricotta, M., Meneghetti, G., Atzori, B., Risitano, G., Risitano, A., 2019. Comparison of Experimental Thermal Methods for the Fatigue Limit Evaluation of a Stainless Steel. Metals (Basel). 9, 677. https://doi.org/10.3390/met9060677

Rigon, D., Ricotta, M., Meneghetti, G., 2019. Analysis of dissipated energy and temperature fields at severe notches of AISI 304L stainless steel specimens. Frat. ed Integrita Strutt. 13, 334–347. https://doi.org/10.3221/IGF-ESIS.47.25

Risitano, A., Fargione, G., Guglielmino, E., 2014. Definition of the linearity loss of the surface temperature in static tensile tests. Frat. ed Integrita Strutt. 30, 201–210. https://doi.org/10.3221/IGF-ESIS.30.26

Risitano, A., Risitano, G., 2013. Determining fatigue limits with thermal analysis of static traction tests. Fatigue Fract. Eng. Mater. Struct. 36, 631–639. https://doi.org/10.1111/ffe.12030

Risitano, G., Clienti, C., 2012. Experimental study to verify the fatigue limit found by thermal analysis of specimen surface in mono axial traction test. Key Eng. Mater. 488–489, 795–798. https://doi.org/10.4028/www.scientific.net/KEM.488-489.795

Risitano, G., Guglielmino, E., Santonocito, D., 2018. Evaluation of mechanical properties of polyethylene for pipes by energy approach during tensile and fatigue tests. Procedia Struct. Integr. 13, 1663–1669. https://doi.org/10.1016/j.prostr.2018.12.348

Vergani, L., Colombo, C., Libonati, F., 2014. A review of thermographic techniques for damage investigation in composites. Frat. ed Integrita Strutt. https://doi.org/10.3221/IGF-ESIS.27.01